79-4054

Experimental Determination of the Artillery Shell Mass-Property/Trajectory-Drift Relationship

L. R. Rollstin*
Sandia Laboratories, Albuquerque, N. Mex.

A series of artillery projectiles with mass-property variations were fired to determine the effect on the trajectory drift. The drift of a spinning projectile is primarily caused by the yaw of repose. Analytic expressions for the repose angle and the drift indicate a dependence on the projectile roll moment of inertia and the center of gravity location and an independence from the projectile pitch moment of inertia. This work provided an experimental verification of these mass-property/drift relationships. Also, a more accurate analytic expression for drift has been developed. This experiment was conducted to enhance the techniques of ballistically matching projectiles when the mass properties cannot be exactly matched. Ballistically matched projectiles under similar firing conditions will impact within specified small dispersion limits.

Nomenclature

C_A = axial-force coefficient
C_{N_a} = normal-force coefficient slope
C_{l_p} = spin-damping coefficient
d = reference diam or diam of projectile
D = drift or crossrange deflection (measured orthogonally from firing azimuth, positive to the right looking downrange)
I_x = roll moment of inertia
I_y, I_z = lateral moment of inertia (symmetry assumed)
I_{xy}, I_{xz} = cross axes moments of inertia
m = mass
M = Mach number
p = projectile spin rate about body x axis
q' = dynamic pressure
$\tilde{q}, \tilde{r}$ or Q, R = nonrolling pitch and yaw rates
S = reference area for aerodynamic coefficients
t = time
U, V, W = velocity components (body fixed axes)
$\tilde{u}, \tilde{v}, \tilde{w}$ = velocity components (relative to the X, Y, Z nonrolling axes)
V_{tot} = body total velocity
X_{cg} = center of gravity distance from nose
X_{cp} = center of pressure (aerodynamic normal force) distance from nose
X', Y', Z' = Earth-fixed coordinate system distances where X' is in direction of range, Y' is in direction of crossrange, and Z' is vertically downward (origin is at gun)
$Y_{\text{cg}}, Z_{\text{cg}}$ = center of gravity offset from longitudinal axis
$\tilde{\alpha}, \tilde{\beta}$ = nonrolling angles of attack and sideslip
$\tilde{\alpha}_R, \tilde{\beta}_R$ = nonrolling yaw of repose angles of attack and sideslip
γ = vertical flight-path angle
θ, ψ, Φ = Euler angles
$\tilde{\xi}$ = $\tilde{\beta} + q\tilde{\alpha}$, complex nonrolling angle of attack
Σ_N = solar aspect angle (between normal to projectile axis and solar vector)
σ = standard deviation

Received June 12, 1978; revision received Sept. 14, 1978.

Index categories: LV/M Configurational Design; LV/M Trajectories and Tracking Systems.

*Member of Technical Staff, Aerodynamics Department. Member AIAA.

Introduction

AN 8-in. gun firing program was conducted to provide an experimental determination of the relationship between the basic mass properties and the crossrange deflection or drift of an artillery projectile. The drift of a spinning artillery shell primarily results from the yaw of repose which develops as the projectile tracks along a curvilinear flight path. Analytical expressions for the yaw of repose and drift of a spinning projectile have been developed by McShane et al.,[1] Murphy,[2] and Vaughn and Wilson.[3,4] The last source primarily addressed the ballistic matching of slightly dissimilar projectiles, i.e., causing the respective mean impacts to be within prescribed dispersion limits. These authors stated that a ballistic match requires that the shells be gyroscopically stable, have similar ballistic coefficients, and develop similar yaw of repose angles during flight.

The analyses indicate that the yaw of repose and drift are primarily dependent on the projectile roll moment of inertia and static margin but essentially independent of the projectile pitch moment of inertia. The purpose of the present test program was to investigate the effects of shell static margin and principal moments of inertia on the yaw of repose and drift to experimentally verify the ballistic match criteria.

Test Preparation

The firing program was conducted at the Tonapah Test Range (TTR), Nevada, using a U.S. Army 8-in. Howitzer (an M201 with a 1-in-20 twist barrel), affixed to a concrete pedestal and fired on a fixed azimuth. This gun and mount arangement essentially removed any firing azimuth dispersion from the crossrange deflection of the projectiles. Inert U.S. Army M106 artillery shells were then modified to give the proper mass property variations for each series of projectiles.

Since the program involved the study of projectile-drift variation with changes in I_x, I_y and X_{cg}, the firing sequence was conducted to include a reference or baseline configuration and two units for each mass property variation. Thus a set of seven projectiles were fired in a continuous series to minimize the variational effects caused by the changing atmospheric conditions.

The test preparation included procedures which aimed at providing constant projectile characteristics and initial flight parameters where no variation was required. Projectile mass properties (except for desired variations), external dimensions, and temperature; gun temperature and firing angle; and gun propellant weight and temperature were all test parameters which were held as constant as possible. A more

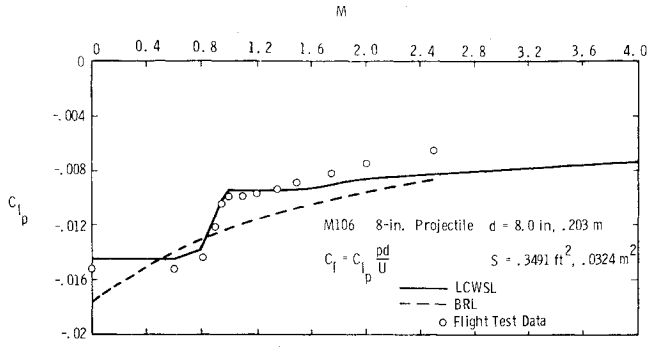

Fig. 1 Spin-damping coefficient vs Mach number.

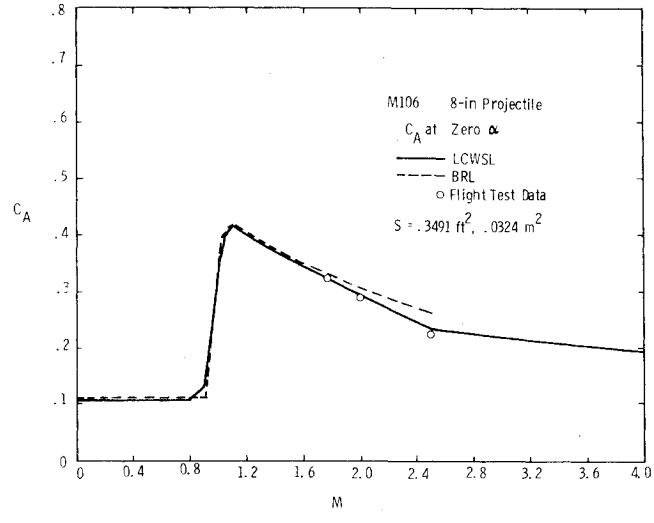

Fig. 2 Axial-force coefficient vs Mach number.

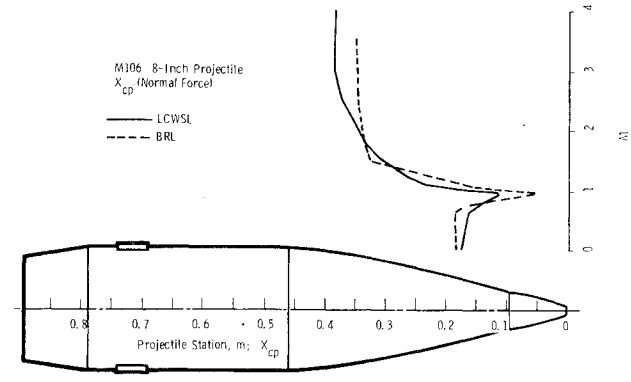

Fig. 3 Normal-force center of pressure vs Mach number.

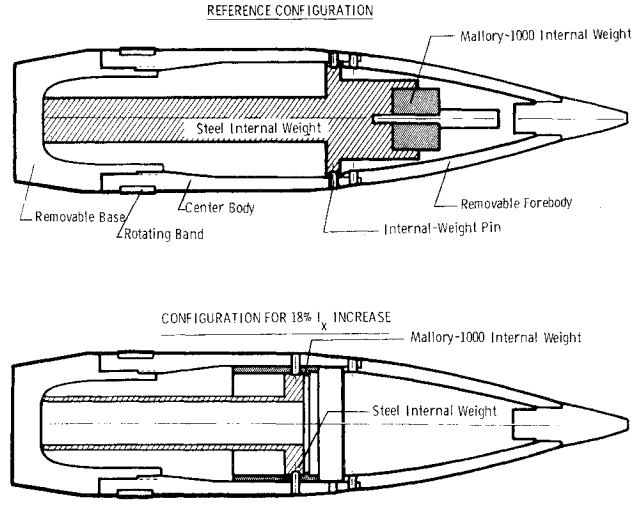

Fig. 4 Sample projectiles in cross section.

complete discussion of these parameters with tolerances is given in Ref. 5.

Aerodynamics

The aerodynamic characteristics of the M106 projectile were obtained in coefficient form from both the Large Caliber Weapons System Laboratory (LCWSL) and the Ballistic Research Laboratory (BRL). Aerodynamic spin-damping coefficient, axial-force coefficient, and normal-force center of pressure data are presented in Figs. 1-3, respectively. Some flight test data obtained during the present firing program are presented for comparison with the estimated aerodynamic coefficients. The spin-damping coefficients obtained from LCWSL were derived from an empirical source, and those from BRL were computed theoretically, but not modified by experiment. Thus the closer agreement was found between the LCWSL coefficients and the current flight data.

Mechanical Design

The mechanical design of the test projectiles required that, to within reasonable tolerances, the external shape be the same, the total mass be constant, and the lateral center of gravity offset and principal axis misalignment be zero. Also, the singular variation of the other mass properties, i.e., roll moment of inertia (I_x), lateral moment of inertia (I_y,I_z), and the center-of-gravity location (X_{cg}), was required to perform the experiment.

Inert, unfilled M106 projectiles were obtained from the U.S. Army to provide the basic structure for each unit. The forward section of each shell was removed at the 0.286-m station to provide access to the interior as well as to allow the replacement nose to be of varying materials and internal configuration. The latter capability allowed larger basic mass property variations to be used which in turn, induced larger trajectory perturbations and hence a more accurate assessment of the sensitivity of the trajectory to each variation. A cross-sectional view of the projectile with maximum I_x as well as that of the reference unit is presented in Fig. 4.

A stress analysis indicated that the wall of the body of the projectile was stressed to near capacity during setback acceleration (10,000 g) without any internal ballast attached to this wall surface. Therefore, all internal ballast configurations were supported on the projectile base. The angular acceleration loads were applied to the added internal structure with pins mounted through the outer wall in longitudinally slotted holes to allow for compressive deflection during setback.

The measured mass properties of the 21 projectiles fired during the test program are presented in Table 1. The rounds in each set are presented in the following order: the reference configuration; the two elevated-I_x projectiles (13 to 18% increase); the two elevated-I_y or elevated-I_z projectiles (11 to 24% increase); and finally the two aft-X_{cg} projectiles (0.29 to 0.36 cal aft movement). The largest lateral center-of-gravity offset measured was 7×10^{-5} m. The largest principal axis misalignment measured was 0.0214 deg.

Test Data Summary

Muzzle Velocity

The projectile velocity at the gun muzzle was measured by two techniques and three data sources. Two Doppler radar sets were used—a Lear-Siegler commercial unit furnished by

Table 1 Projectile mass properties

Test number	Mass, kg	X_{cg}, m	Moments of inertia, kg m^2 I_x	I_y	I_z
09	91.36	0.592	0.4735	3.845	3.845
10	91.39	0.590	0.5401	3.865	3.866
11	91.36	0.592	0.5577	3.880	3.881
12	91.42	0.592	0.4750	4.281	4.279
13	91.63	0.591	0.4745	4.758	4.758
14	91.32	0.666	0.4752	2.867	2.863
15	91.49	0.652	0.4767	3.911	3.913
18	91.47	0.592	0.4829	3.857	3.849
19	91.39	0.592	0.5480	3.872	3.879
20	91.25	0.593	0.5531	3.871	3.871
21	91.46	0.592	0.4754	4.288	4.288
22	91.36	0.593	0.4748	4.717	4.717
23	91.37	0.666	0.4753	2.866	2.867
24	91.54	0.653	0.4804	3.902	3.907
27	91.40	0.593	0.4741	3.845	3.845
28	91.40	0.592	0.5481	3.872	3.879
29	91.24	0.592	0.5529	3.871	3.871
30	91.45	0.592	0.4758	4.285	4.285
31	91.43	0.592	0.4743	4.714	4.711
32	91.31	0.666	0.4751	2.858	2.859
33	91.55	0.652	0.4799	3.902	3.907

the BRL and a Sandia Laboratories prototype set. Also, image-motion film was obtained and the projectile-image length measured to determine the velocity. The Lear-Siegler Doppler radar was used as the source of final data. Some minor adjustments were made to the prototype set during the firing of the first group of projectiles. The two Doppler radars were in agreement within 1.5 m/s during the 14 remaining firings. The velocity determined from the image motion film averaged 6.2 m/s lower than that of the Doppler data (standard deviation from this mean difference was 1.8 m/s). The reason for this bias was not evident, but may have resulted from a small (~0.8%), but consistent error in the application of timing marks on the film. Since the radar data were consistent and were generated by using separate systems, they were assumed to be the more accurate. The average muzzle velocity for the 21 data rounds was 787.2m/s with a standard deviation of 1.4 m/s.

Atmospheric Measurements

A series of meterological soundings at 1-h time intervals was conducted during the test program so that the atmospheric conditions for each round could be estimated and applied to the postfiring trajectory simulation. Since the wind profile was more variable than the other meterological parameters and had a significant influence on the projectile trajectory, wind balloons were alternated with rawinsonde balloons. The former carried only a radar reflector as compared to the latter which included a reflector and a rawinsonde instrument which collects data on other atmospheric parameters. Thus the wind profile was measured during each sounding and the remaining meterological data were obtained every other sounding. The firing program was purposely conducted during stable weather conditions, i.e., during a period well removed from weather frontal activity. However, atmospheric conditions still exhibited slow variations caused by the large-scale movement of air masses and by diurnal effects. Therefore, the atmopheric conditions for each round were estimated by interpolating the various sounding data at each fire time with altitude as the independent variable.

Gun Pressure

The gun breech pressure was measured by using crush gauges and transducers. It is of interest to note that there appeared to be a slight trend of rising maximum pressure as the time between rounds increased from 11 to 20 min. The rise appeared to be appoximately 3.5% of the average maximum breech pressure at the 11-min wait time. The trend of the data outside this wait-time span is unknown since only one data point exists outside this range. It is possible that an optimum time between rounds does exist, if the largest breech pressure maximum is required.

Trajectory

The actual trajectory for each projectile was measured by C-band instrumentation radars in the skin-track mode. An uprange radar provided tracking data for the major portion of each flight (inaccuracies usually became evident at an elevation of 4 km above ground level during descent). A downrange radar provided terminal tracking to impact and assisted a ground party in locating the impact point of each round. A typical trajectory is presented in Fig. 5. This figure illustrates the radar tracks, six-degree-of-freedom (6DOF) trajectory simulation, and the surveyed impact location.

Input to the 6DOF code included measured projectile mass properties, muzzle conditions, and meterological data (including winds) for each round. Since the code used included a nonrotating Earth model, an average Coriolis acceleration correction was applied to the computed trajectories. The magnitude of this correction at impact was 166 m in drift and −45 m in range. The 6DOF code provided an accurate simulation of each round. The average difference between the simulated and actual impact ranges was 19 m with a standard deviation of 57 m. The average impact drift difference was 5 m with a standard deviation of 34 m.

Analytical Method for Drift

The expression for the yaw of repose of a spinning projectile as written by Vaughn and Wilson[3] is

$$\tilde{\beta}_R = \frac{pI_x\dot{\gamma}}{C_{N_\alpha} q' S(X_{cg} - X_{cp})} \tag{1}$$

The corresponding equations from Refs. 1 and 2 are the same except that the vacuum-trajectory expression for the flight

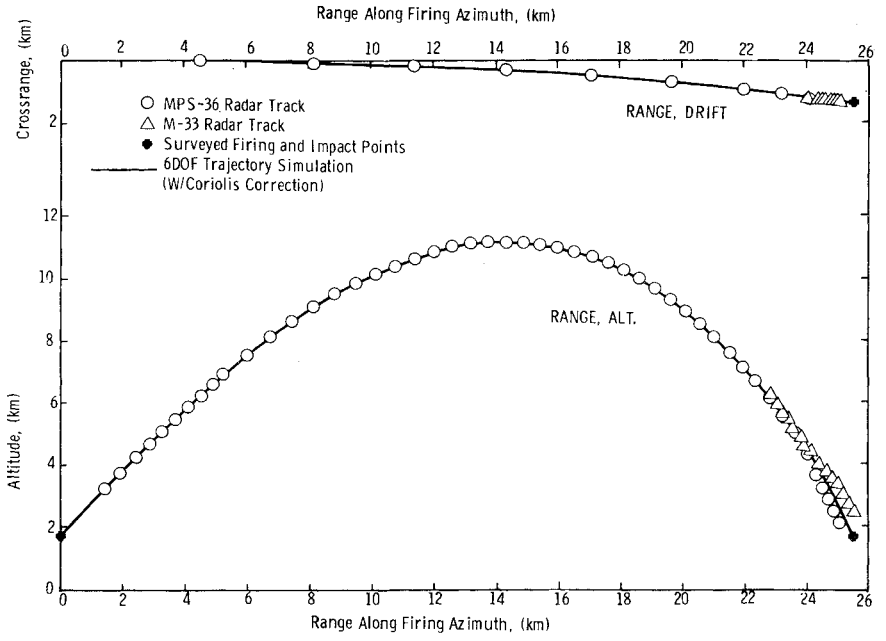

Fig. 5 Trajectory for projectile 27.

path angle, γ, is used. Equation (1) is applied in the following development of the drift equation.

Previously developed equations for the drift of a spinning projectile[1,3] overestimate this trajectory deflection. The drift at impact for a trajectory typical of the present study was overpredicted by as much as 55% using the previous expressions as compared to a 6DOF trajectory simulation. The need for a more precise expression for the drift appeared evident and is developed below.

An expression for the lateral velocity or drift rate in the Earth-fixed axes system and the body-Euler angles is written by Etkin[6] as

$$\frac{dY'}{dt} = U\cos\theta\sin\psi + V(\sin\Phi\sin\theta\sin\psi + \cos\Phi\cos\psi) + W(\cos\Phi\sin\theta\sin\psi - \sin\Phi\cos\psi) \quad (2)$$

The assumptions that 1) a nonrolling aeroballistic axes system for the body causes Φ to be zero; 2) for the nonrolling axes system, $\tilde{w}$ remains small compared to $\tilde{u}$ and $\tilde{v}$ (velocity components along nonrolling axes); and 3) ψ remains small (less than 10 deg); reduce Eq. (2) to

$$dY'/dt = \tilde{u}(\cos\theta)\psi + \tilde{v} \quad (3)$$

Also, from Etkin[6]

$$\dot{\psi} = (Q\sin\Phi + R\cos\Phi)\sec\theta$$

Using the above assumptions, this equation reduces to

$$\dot{\psi} = (1/\cos\theta)R \quad (4)$$

An expression for R or $\tilde{r}$, the nonrolling yaw rate (about the z axis), is now developed. The complex nonrolling lateral rate $\tilde{\zeta}$, as written by Hodapp,[7] is

$$\tilde{\zeta} = -i\dot{\tilde{\xi}} + i\left(\frac{q'S}{mU}\right)(C_A - C_{N_\alpha})\tilde{\xi}$$

$$+ \frac{ip^2(Y_{cg} + iZ_{cg})e^{2pt}}{U} - q\frac{\cos\theta}{U} = \tilde{q} + i\tilde{r}$$

Thus, with no center of gravity offsets

$$\tilde{r} = R = -\dot{\tilde{\xi}} + (q'S/mU)\left(C_A - C_{N_\alpha}\right)\tilde{\xi}$$

where $\tilde{\xi} = -\tilde{\beta} + i\tilde{\alpha}$, the complex nonrolling angle of attack.

The $\tilde{\alpha}$ and $\tilde{\beta}$ for a well-balanced, symmetrical, spin-stabilized projectile are approximately equal to $\tilde{\alpha}_R$ and $\tilde{\beta}_R$, the angle of attack and yaw of repose. Also, $\tilde{\beta}_R \cong 20\tilde{\alpha}_R$ (see Vaughn and Wilson[3]) and is, thus, the dominant component. Therefore,

$$R \simeq -\dot{\tilde{\beta}}_R + (q'S/mU)\left(C_A - C_{N_\alpha}\right)\tilde{\beta}_R \quad (5)$$

Since $\tilde{\alpha}_R$ is small, the vertical flight-path angle and the body-pitch Euler angle are nearly equal ($\gamma \cong \theta$). Also, the velocity along the body x axis and the body total velocity are nearly equal ($V_{tot} \cong \tilde{u}$). If Eq. (5), with the above approximations, is applied to Eq. (4), it becomes

$$\dot{\psi} = \frac{1}{\cos\gamma}\left[-\dot{\tilde{\beta}}_R + \left(\frac{q'S}{mV_{tot}}\right)\left(C_A - C_{N_\alpha}\right)\tilde{\beta}_R\right]$$

If this expression is integrated and the following are substituted

$$\tilde{\beta}_R \simeq \beta = \tan^{-1}\tilde{v}/\tilde{u} \cong \tilde{v}/\tilde{u}$$

$$\tilde{v} \simeq \tilde{u}\tilde{\beta}_R \simeq V_{tot}\tilde{\beta}_R$$

the drift rate, Eq. (3), becomes

$$\frac{dD}{dt} = V_{tot}\cos\gamma\int_0^t \frac{1}{\cos\gamma} \times\left[-\dot{\tilde{\beta}}_R + \frac{q'S}{mV_{tot}}\left(C_A - C_{N_\alpha}\right)\tilde{\beta}_R\right]dt + V_{tot}\tilde{\beta}_R$$

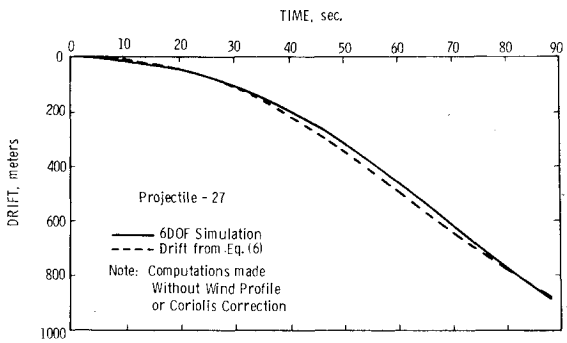

Fig. 6 Comparison of drift computations.

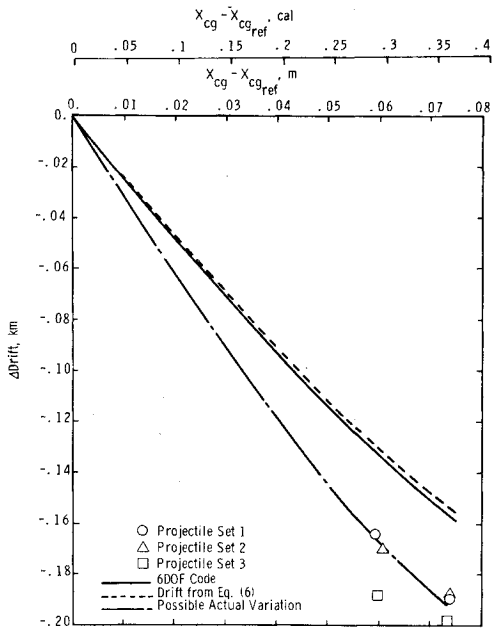

Fig. 7 Effect of center-of-gravity position on projectile drift at impact.

If the expression for the yaw of repose, Eq. (1), is substituted into this drift-rate equation, and the result is integrated, the final equation for deflection is obtained

$$D=\int_0^t V_{\text{tot}}\left\{\cos\gamma\int_0^t \frac{1}{\cos\gamma}\left[-\frac{\mathrm{d}}{\mathrm{d}t}\frac{pI_x\dot{\gamma}}{C_{N_\alpha}q'S(X_{\text{cg}}-X_{\text{cp}})}\right.\right.$$

$$+\frac{q'S}{mV_{\text{tot}}}\left(C_A-C_{N_\alpha}\right)\frac{pI_x\dot{\gamma}}{C_{N_\alpha}(X_{\text{cg}}-X_{\text{cp}})}\Bigg]\mathrm{d}t$$

$$\left.+\frac{pI_x\dot{\gamma}}{C_{N_\alpha}q'S(X_{\text{cg}}-X_{\text{cp}})}\right\}\mathrm{d}t \qquad (6)$$

The trajectory deflection as calculated using Eq. (6) is compared with a 6DOF computation for round 27 of the present test series in Fig. 6.

Test Results

The purpose of the M106 yaw of repose gun firings was to verify experimentally that variations of the projectile roll moment of inertia and center of gravity position do cause changes in projectile drift. Also, a demonstration of drift insensitivity to changes in the projectile pitch moment of

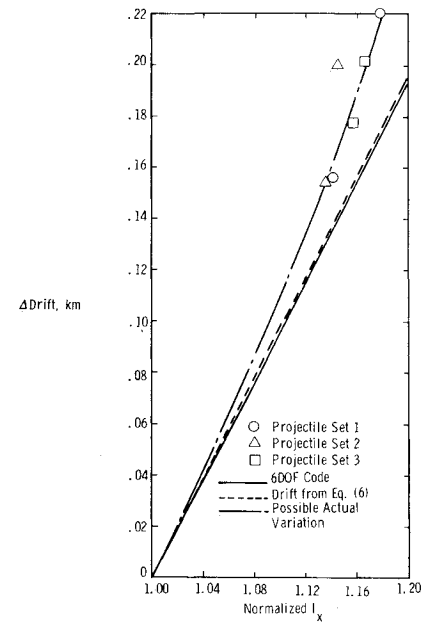

Fig. 8 Effect of axial moment of inertial on projectile drift at impact.

inertia was desired. Three sets of the seven configurations were fired during this test program. Figures 7 and 8 illustrate the differences in drift at impact as a function of I_x ratio and X_{cg} shift. The flight-test data have been adjusted and normalized to isolate the drift changes caused by the controlled mass property variations. The computed wind effects (6DOF simulations with and without measured wind profile) were removed from the range and drift data for each round. The secondary drift effects for small variations of I_x and X_{cg} from the reference, where no such variations were intended, have also been removed. The drift sensitivities for this normalization were based on 6DOF simulations. Since maximum corrections of 15 and 5 m were calculated for unintentional I_x and X_{cg} variations, respectively, the simulations provided adequate sensitivity. The impact drift data were also normalized with respect to the range at impact. Since there was some impact range dispersion (primarily caused by muzzle velocity variation), each impact range point was normalized to that of the corresponding reference round. This range adjustment produced a drift change (maximum of 23 m) since the horizontal flight-path angle near impact was not zero. Some range variation does occur with intended I_x and X_{cg} variation as simulated by the 6DOF trajectory computation. These predicted range effects were not removed as the impact range was normalized.

The same adjustment and normalization techniques were also applied to the impact data for the I_y variation projectiles. These projectiles from the first and third sets yielded 4 m or less variation in drift from that of the reference round with I_y increases as high as 23%. The two second-set I_y variation units averaged a drift increase of 23.5 m with respect to the reference. However, all the off-reference rounds of the second set of projectiles appeared to have a drift-difference bias of approximately 25 m. This bias may have been caused by a mislocation of the second-set reference round during the impact-point survey or perhaps by some test anomaly for the same round which is not evident in the flight data. It should be noted that this apparent bias was removed before final drift data analysis.

The drift sensitivity as determined from 6DOF simulations and from Eq. (6), is also presented in Figs. 7 and 8. The data were underpredicted for both mass property variations. The trajectory time history of these differences between predicted and actual drift is illustrated in Fig. 9. The data showed

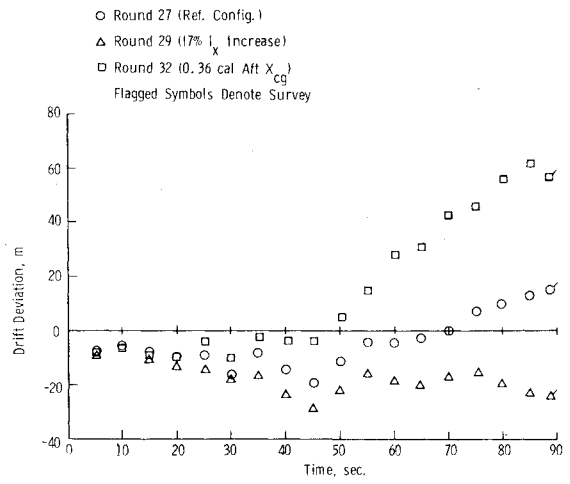

Fig. 9 Comparison of six-degree-of-freedom simulation to radar track and impact survey.

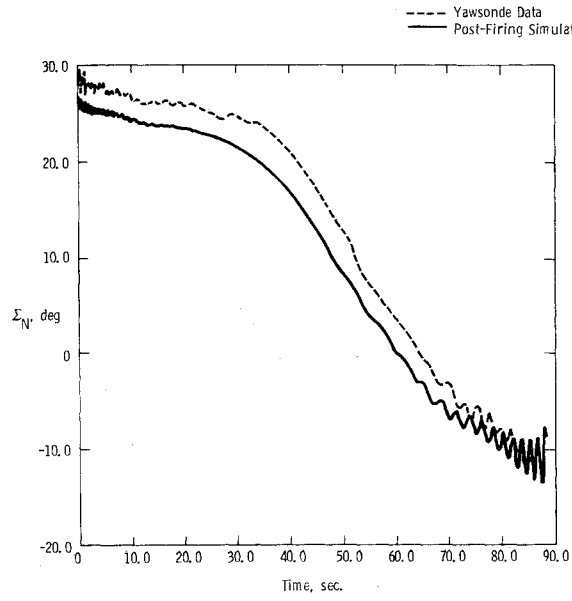

Fig. 10 Sun-angle history for round 33.

essentially no configurational variation for the first 15 s of flight. The consistent deviation which appeared for all three rounds over this time period may have been caused by a small firing azimuth error (~ 0.1 deg) or a gun location error of approximately 7 m. The azimuthal error seems more likely and could result from a gun platform tilt as small as 0.07 deg or from a gun barrel dynamic effect which provides a consistent off-nominal initial flight condition independent of projectile configuration. The deviation which was related to projectile mass property configuration appeared to begin at approximately 20 s. The most significant change in the drift differences began between 35 and 45 s (apogee is near 40 s, maximum yaw of repose occurs from 40 to 45 s.) Apparently, no significant relative change occurred between the actual and simulated yaws of repose since there was no significant relative change observed between the simulated and actual sun angle† (see Fig. 10). Therefore, the deviation in drift trends near apogee could be caused by poor simulation of the projectile aerodynamics in the transonic flight regime ($M = 1.0$ usually occurs between 35 and 40 s during ascent). Nonlinear effects seem most likely since the 6DOF aerodynamic inputs were linear and the varying mass properties produced a yaw of repose variation (range of repose angle maximum was from 2 to 3 deg for minimum- and maximum-drift rounds, respectively).

†The actual sun angle was measured on four rounds (28, 29, 30, 32) using a yawsonde device attached to the nose of the projectile (see Mermagen[8]).

Ballistic Matching

The task of ballistically matching slightly dissimilar spin-stabilized projectiles, i.e., causing them to fly similar trajectories, involves the matching of many projectile parameters. Although the drift of a projectile off the firing azimuth is significant, the amount relative to the projectile range is still small (a factor of 1/25 for the maximum-range condition of the 8-in. shells considered here). Thus the time history of range and altitude of two projectiles can be closely matched with no consideration of drift parameters. If the initial or muzzle conditions (velocity, flight-path angle, elevation above terrain), the projectile mass, and the projectile external shape (specifically the aerodynamic drag) are nearly the same, then the range and altitude-time histories of the two shells will be similar. The range and altitude parameters which appear in the expression for drift developed above are V_{tot}, γ, q', and M.

The remaining parameters in Eq. (6) relate directly to the drift of the shell and, of course, must be approximately the same or must at least balance for a complete ballistic match to be realized. These parameters are p, I_x, C_{N_α}, $X_{cg} - X_{cp}$, m, and C_A. If the range and altitude parameters have been matched, the roll-rate time history will also be matched because of similar muzzle velocity from the same gun and because of similar spin damping (external-shape match). Similarities in range trajectory and external shape would also assure the similarity of projectile mass, C_A, C_{N_α}, and X_{cp}. Therefore, only the $I_x/(X_{cg} - X_{cp})$ term remains for consideration. Of course, the X_{cp} history is fixed by the external shape, leaving the I_x and X_{cg} parameters to provide for trajectory matching between two slightly dissimilar projectiles.

A ballistic match can be assured if the differential drift caused by a center-of-gravity variation between two projectiles is offset by an equal and opposite differential drift generated by dissimilar roll moments of inertia. The sensitivity of drift to an X_{cg} or I_x change for a given projectile can be determined through experiment or estimated by using a 6DOF simulation or Eq. (6).

Conclusion

The dependency of the drift of a spinning artillery shell on the shell's roll moment of inertial (I_x) and center of gravity position (X_{cg}) has been experimentally verified. Also, it has been shown that the drift is essentially independent of the shell's pitch moment of inertia (I_y). However, the magnitude of the drift difference with an I_x or X_{cg} variation was not well predicted by the 6DOF trajectory simulations (aproximately 20% error) for the M106 projectile. Further study to determine the reason for this discrepancy is recommended. The problem may stem from inaccuracies in the aerodynamic characteristics input for the M106.

An analytical expression for drift has been developed that compares well with 6DOF simulations. This drift equation illustrates the relationship of the drift to the projectile I_x and X_{cg} and the independence of drift from I_y.

The firing program described herein should help establish the fact that two projectiles with dissimilar mass properties can be ballistically matched. The I_x and X_{cg} of the shell to be matched can be tailored to produce the same drift as that of the reference, or standard, round.

Acknowledgments

The author wishes to acknowledge the contribution of V. Oskay of the BRL to this test program. The field support and data-reduction efforts with the Lear-Siegler Doppler radar and the yawsonde devices given by V. Oskay and the BRL were greatly appreciated. The mechanical design of the projectiles fired during this test program was accomplished by R. D. Fellerhoff of Sandia Laboratories. This work was supported by the Department of Energy.

References

[1]McShane, E. J., Kelley, J. L., and Reno, F. V., *Exterior Ballistics,* University of Denver Press, Denver, Colo., 1953.

[2]Murphy, C. H., "Free Flight Motion of Symmetric Missiles," Ballistic Research Laboratories, Aberdeen Proving Ground, Md., Rept. 1216, July 1963.

[3]Vaughn, H. R., and Wilson, G. G., "Yaw of Repose on Spinning Shells," Sandia Laboratories, Albuquerque, N.Mex., SC-RR-70-155, Jan. 1970.

[4]Vaughn, H. R. and Wilson, G. G., "Effect of Yaw of Repose on Ballistic Match of Similar Projectiles," *AIAA Journal,* Vol. 9, June 1971, pp. 1208-1210.

[5]Rollstin, L. R., "Experimental Determination of the Effect of the Basic Mass Properties on the Drift of an Artillery Shell," Sandia Laboratories, Albuquerque, N. Mex., SAND78-0008, April 1978.

[6]Etkin, B., *Dynamics of Flight,* Wiley, New York, 1959.

[7]Hodapp, Jr., A. E., "Effect of Mass Asymmetry on Ballistic Match of Projectiles," Sandia Laboratories, Albuquerque, N. Mex., SAND77-0324, March 1977.

[8]Mermagen, W. H., "Measurements of the Dynamical Behavior of Projectiles Over Long Flight Paths," *AIAA Journal,* Vol. 8, April 1971, pp. 380-385.